

# Generation of 64-fs L-band stretched pulses from an all-fibre Er-doped laser

ZINAN HUANG,<sup>1</sup> SONIA BOSCOLO,<sup>2</sup> QIANQIAN HUANG,<sup>1</sup> ZHIKUN XING,<sup>3</sup> ZHIJUN YAN,<sup>3</sup> TAO CHEN,<sup>4</sup> YUNQI LIU,<sup>1</sup> AND CHENGBO MOU<sup>1,\*</sup>

<sup>1</sup>Key Lab of Specialty Fiber Optics and Optical Access Network, Shanghai Institute for Advanced Communication and Data Science, Joint International Research Laboratory of Specialty Fiber Optics and Advanced Communication, Shanghai University, Shanghai 200444, China

<sup>2</sup>Aston Institute of Photonic Technologies, School of Engineering and Applied Science, Aston University, Birmingham B4 7ET, UK

<sup>3</sup>National Engineering Laboratory for Next Generation Internet Access System, School of Optical and Electronic Information, Huazhong University of Science and Technology, Wuhan 430074, China, and also with the Wuhan National Laboratory for Optoelectronics, Huazhong University of Science and Technology, Wuhan 430074, China

<sup>4</sup>Key Laboratory of Space Active Opto-Electronics Technology, Shanghai Institute of Technical Physics, Chinese Academy of Sciences, Shanghai 200083, China

\*mouc1@shu.edu.cn

**Abstract:** We demonstrate an L-band all-fibre erbium-doped laser mode locked by nonlinear polarisation rotation and working in the stretched-pulse regime. The use of a single segment of gain fibre with appropriate length and dispersion and a Brewster fibre grating optimised for the L band as an in-fibre polariser enables the generation of pulses at 1.59- $\mu$ m central wavelength, which can be linearly compressed to 64-fs duration. Numerical simulations of the laser model support our experimental findings. Our laser design gives a route towards low-cost and low-complexity fibre-integrated laser sources for applications requiring L-band ultrashort pulses.

Published by The Optical Society under the terms of the [Creative Commons Attribution 4.0 License](https://creativecommons.org/licenses/by/4.0/). Further distribution of this work must maintain attribution to the author(s) and the published article's title, journal citation, and DOI.

## 1. Introduction

Driven by potential applications that range from optical communications to materials characterisation, the development of ultrashort-pulse sources remains one of the most active areas of laser development. Passively-mode-locked fibre lasers have been the subject of considerable research interest for several decades because they can realise reliable and cost-effective compact ultrafast light sources [1,2]. Recent years have seen growing interest in ultrashort-pulse erbium-doped fibre (EDF) lasers operating in the L band (1565 to 1625 nm), owing to their capability to expand the band of telecommunications and sensing [3,4], and their various applications in spectroscopy, biomedical diagnostics and surgery, where scattering and self-focusing effects are significantly reduced by shifting the laser wavelength into the L band [5,6]. Although the typical gain window of EDFs is located in the C band (1530 nm to 1565 nm), a moderate population inversion in the EDF (30% to 40%) permits to obtain a positive gain at 1600 nm [6]. A simple way to limit the population inversion in a laser is to control the linear losses of the cavity [7] and based on this principle, a number of studies on L-band mode-locked EDF lasers have been reported [8–10]. However, these lasers operate in the soliton regime and, thus, the pulse duration and energy are constrained [2].

To obtain shorter pulse durations, larger spectral widths and higher pulse energies from fibre lasers, various nonlinear mechanisms of pulse generation besides the soliton concept have been

proposed. These include stretched pulses (or dispersion-managed solitons) [11,12], self-similar pulse (similariton) propagation and all-normal or strong-net normal dispersion regimes [13]. In particular, in a laser in which the net cavity dispersion is designed to be close to zero by including segments of normal and anomalous group-velocity dispersion (GVD), a pulse will stretch and compress periodically, and the nonlinear phase is exactly balanced by the net effect of dispersion, thus enabling significant reduction (increase) of the achievable pulse duration (energy) compared to a soliton laser. The short pulse duration and small cavity dispersion magnitude of such a stretched-pulse regime result in a lower level of timing jitter and relative intensity noise than other mode-locked regimes such as soliton or similariton [14]. Generation of pulses with femtosecond durations has been demonstrated in stretched-pulse lasers mode-locked by different techniques, such as nonlinear polarisation rotation (NPR) [15], figure-of-eight cavity configuration [16] or material-type saturable absorbers [17,18]. The stable mode-locked operation and output pulse characteristics in a stretched-pulse laser depend not only on the net cavity dispersion but also on the parameters of the mode-locking element [19]. Therefore, owing to its fast recovery time and large modulation depth, the NPR method based on the intrinsic Kerr nonlinearity of optical fibres still remains a major solution for the generation of sub-100-fs pulses [15,20–22]. To date, the 34.3-fs pulses reported in [22] are the shortest pulses available directly from an EDF oscillator. However, the majority of the stretched-pulse lasers demonstrated so far operate in the C band. Furthermore, their NPR settings include free-space polarising elements and waveplates, which sacrifice the benefits of high stability, compactness and ease of integration which are intrinsic to the all-fibre format.

Whilst lengthening the EDF can force the laser to emit in the L band [3,23,24], the extra losses introduced by an overlong EDF make it difficult for the laser to achieve stable mode locking and also make NPR-based lasers more sensitive to the environment. Moreover, in lasers operating at net normal dispersion, large bandwidths and high pulse energies are favoured by short fibre cavities. Sub-90-fs and sub-60-fs L-band pulses have been obtained from all-fibre erbium-doped lasers exploiting the dissipative-soliton and similariton pulse formation mechanisms, respectively [25,26]. However, such laser designs require two segments of different types of EDFs to force the laser to operate at 1.6  $\mu\text{m}$ , hence two pump diodes, and bidirectional pumping, which adds on implementation complexity and cost and reduces efficiency [27].

To realise an all-fibre L-band stretched-pulse laser with a simple structure, the challenge lies in the appropriate selection of the EDF length and dispersion and of the polarisation element, as well as in the management of the in-cavity nonlinearity. Brewster fibre gratings based on a 45°-tilted structure have been extensively used as effective in-fibre polarisers in mode-locked fibre lasers working in different pulse shaping regimes and spectral bands [28–33]. In this paper, we demonstrate the generation of pulses at 1591-nm central wavelength and linearly compressible to 64-fs duration from an all-fibre stretched-pulse erbium-doped laser. The laser uses a Brewster fibre grating optimised for the L band and only one section of EDF to compensate the in-cavity dispersion while forcing emission in the L band. Numerical simulations of the laser model confirm the stretched-pulse regime observed in the experiments. The laser design is simple and suitable for all-fibre integration.

## 2. Laser configuration and principle

The schematic diagram of the L-band stretched-pulse mode-locked EDF laser is illustrated in Fig. 1(a). In order to achieve a net cavity dispersion near zero and force the laser to emit in the L band while maintaining the simplicity of the laser design, a 1.575-m section of high dopant-concentration EDF with a nominal absorption coefficient of  $\sim 80$  dB/m at 1530 nm and a GVD of  $-45.1$  ps/(nm·km) at 1590 nm is selected as the gain medium. The EDF is forwardly pumped through a fused 980/1550-nm wavelength division multiplexer by a commercial laser diode operating at 976 nm and providing up to 704-mW pump power. We note that since in our

experiment we relied on intra-band absorption to generate L-band laser light, the gain fibre and pump power were not particularly optimised. Other fibres in the cavity are standard single-mode fibre (SMF) with a GVD of +19.4 ps/(nm·km) at 1590 nm, yielding a small normal cavity dispersion which triggers operation of the laser in the stretched-pulse regime [11]. A Brewster fibre grating with strong polarisation-dependent loss (PDL) sandwiched with two polarisation controllers (PCs), converts NPR to amplitude modulation, initiating and stabilising mode-locked operation [29]. A polarisation-independent isolator ensures single direction oscillation. A fibre coupler after the EDF taps 40% of laser power out of the cavity for measurement. The location of the output coupler (OC) along with minimisation of the length of the coupler's leading fibre facilitates the achievement of a wide output spectrum and the use of SMF (coupler's pigtail) for pulse compression outside the cavity. Further, this output coupling position may help reduce detrimental nonlinear effects induced by the relatively long EDF in the cavity. An optical spectrum analyser (Yokogawa AQ6370B), a radio-frequency (RF) analyser (SIGLENT SSA 3032X), an auto-correlator (Femtochrome FR-103XL), and a 12.5 GHz fast photodetector (Newport 818-BB-51F) connected to an 8-GHz oscilloscope (Keysight DSO90804A) are used to characterise the laser output.

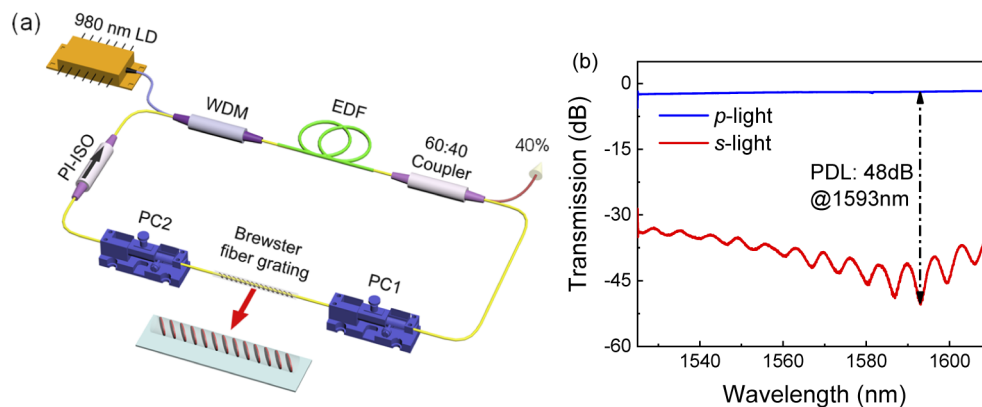


**Fig. 1.** (a) Experimental setup of the L-band stretched-pulse mode-locked fibre laser. LD: laser diode, WDM: wavelength-division multiplexer, EDF: erbium-doped fibre, PC: polarisation controller, PI-ISO: polarisation-independent isolator. (b) Insertion loss of the Brewster fibre grating measured at two orthogonal polarisation states.

The Brewster fibre grating is inscribed into a length of hydrogenated SMF by ultraviolet laser light using the standard phase mask scanning technique. A description of the operation principle and fabrication procedure can be found in [34]. A commercial optical vector analyser (LUNA, OVA5000) incorporating a tunable laser is used to acquire the transmission characteristics of the grating over the spectral range 1525 nm to 1610 nm (with 1.6-pm resolution). The key property of the grating as a polarisation-dependent device is its PDL, which is defined as the peak-to-peak difference in transmission with respect to all possible states of polarisation. This can be then measured as the ratio of the maximum to the minimum insertion loss occurring at two orthogonal polarisation states, as shown in Fig. 1(b). It is seen that the grating features a PDL of ~48 dB at 1593 nm, while the PDL remains well above 35 dB over a wide range of the L band. The study reported in [35] indicates that Brewster gratings with high PDL are advantageous to achieving short pulses at a low pump threshold and high power-conversion efficiency. Therefore, the strong grating's PDL drives the generation of ultrashort pulses in our laser setup, while the relatively long EDF length permits to acquire L-band emission. The oscillation observable in the loss profile of the *s*-light is due to the back reflection of radiation modes at the boundary between the fibre cladding and air, thereby forming the cladding mode oscillation [36]. However, this

oscillation has no observable effect on the mode-locking performance of the laser and can be eliminated by immersing the grating in a medium with a refractive index similar to that of the fibre cladding [36]. We can also see in Fig. 1(b) that the insertion loss of the  $p$ -light is relatively small, with values not exceeding 2 dB across the entire L band.

### 3. Results and discussion

Through management of the cavity dispersion realised by finely tuning the length of the in-cavity SMF, we found that the optimal cavity length is 5.02 m, yielding a net dispersion of  $\sim 0.006$  ps<sup>2</sup> at 1590 nm. Under this cavity length, mode-locked operation of the laser can be easily obtained when the pump power is above 150 mW by properly adjusting the PCs.

The performance of the laser at 200-mW pump power is summarised in Fig. 2. The output pulse train as observed on the oscilloscope (Fig. 2(a)) shows a pulse spacing of  $\sim 24.6$  ns, yielding a repetition rate of  $\sim 40.63$  MHz. The average output power from the laser is 16.5 mW, corresponding to a pulse energy of 0.41 nJ. The RF spectrum of the laser output measured with a resolution of 1 kHz over a 1-MHz band around the cavity fundamental frequency (Fig. 2(b)) features a signal-to-noise ratio of 58.4 dB. The low noise background in the RF spectrum over a 3.2-GHz range with a 10-kHz resolution (inset of Fig. 2(b)) also provides evidence of stable single-pulse mode-locking operation. The corresponding Kelly sideband-free, wide optical spectrum profile shown in Fig. 2(c) is a signature of the stretched-pulse operation regime [11]. The spectrum, measured with a 0.05-nm resolution, is centred on 1591 nm and has a bandwidth at full width at half-maximum (FWHM) of 65.1 nm. The inset in Fig. 2(d) shows the measured autocorrelation trace of the direct output pulse indicating a FWHM pulse duration of 240 fs when a Gaussian fit is assumed. By optimising the SMF pigtail of the laser output port, the pulse can be compressed to 64-fs duration (Fig. 2(d)). This gives a time-bandwidth product of 0.49, which is very close to the Fourier transform limit for a Gaussian pulse (0.441). These pulses are the shortest pulses generated so far in the L band from a fibre laser using a single segment of EDF. With the linear (dispersive) pulse compression method used here, the small pedestals in the autocorrelation trace of the compressed pulse are a signature of uncompensated higher-order dispersion and nonlinear chirp [15].

We note that steady operation of the laser could be maintained for at least 10 hours after mode locking occurred, under laboratory conditions and in the absence of external disturbance. We also note that increasing the pump power beyond 200 mW resulted in multiple pulse formation in the laser as a result of a peak-power-limiting effect of the laser cavity [37].

To support our experimental observations, we have performed numerical simulations of the laser using the same configuration as the experimental setup. Propagation within the fibre sections is modelled with a standard modified nonlinear Schrödinger equation (NLSE) [38]:

$$i\psi_z - \frac{1}{2}\beta_2\psi_{tt} + \gamma|\psi|^2\psi = \frac{i}{2}g\left(\psi + \frac{1}{\Omega^2}\psi_{tt}\right) \quad (1)$$

where  $\psi = \psi(z, t)$  is the slowly varying amplitude of the pulse envelope,  $z$  and  $t$  are the propagation and time delay parameters,  $\beta_2$  is the GVD parameter and  $\gamma$  is the coefficient of cubic nonlinearity of the fibre. The dissipative terms in (1) represent linear gain as well as a parabolic approximation to the gain profile with the bandwidth  $\Omega$ . The gain  $g$  is saturated according to  $g(z) = g_0/(1 + W/W_0)$ , where  $g_0$  is the small-signal gain, which is non-zero only for the gain fibre,  $W(z) = \int dt|\psi|^2$  is the pulse energy, and  $W_0$  is the gain saturation energy determined by the pump power. The NPR mode-locking regime for the sake of clarity is modelled by a simple transfer function [37]:  $T = 1 - q_0/[1 + P(t)/P_0]$ , where  $q_0$  is the unsaturated loss due to the saturable absorber,  $P(z, t) = |\psi(z, t)|^2$  is the instantaneous pulse power, and  $P_0$  is the saturation power. Linear losses are imposed after the EDF segment, which summarise intrinsic losses and output coupling. The parameters used in the numerical simulations are similar to their nominal

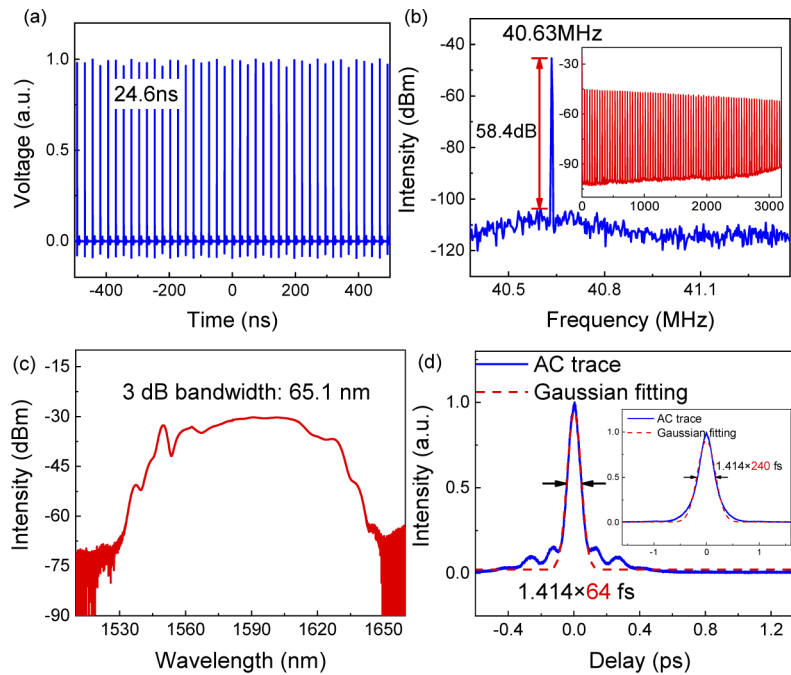


**Fig. 2.** Mode-locked operation of the laser at 200-mW pump power. (a) Output pulse train. (b) RF spectrum. (c) Optical spectrum. (d) Autocorrelation traces of the compressed and direct output (inset) pulses, and corresponding Gaussian fits (dashed red curves).

or estimated experimental values (see [Supplement 1](#) for details). We would like to point out that we do not aim here at a comprehensive comparison of numerical modelling and experiments and intentionally consider a simplified description of some key effects. Instead, we use this simple model to verify the main features of the generated pulse propagation regime. The numerical model is solved with a standard symmetric split-step propagation algorithm, and the initial field is a weak noisy signal.

The pulse evolution is illustrated by plots of the FWHM pulse duration and spectral bandwidth and the root-mean-square (rms) chirp parameter (defined so that to be  $C$  if the pulse is of the form  $\psi = A(t)e^{iCt^2}$ ) as a function of position in the cavity in [Fig. 3](#). We can clearly see that the laser operates in the stretched-pulse regime (see [Supplement 1](#) for details) [12]: the pulse temporally stretches and compresses twice per round-trip, reaches a minimum duration in the middle of the EDF and SMF segments, and acquires both signs of chirp. The calculated temporal and spectral breathing ratios are approximately 43.4 and 8.6, respectively. It is worth noting that although the largest width of the spectrum is attained in the middle of the SMF segment, at this cavity position the spectrum features a highly oscillatory structure arising from self-phase modulation. The spectral bandwidth at FWHM of the output pulse ([Fig. 4\(b\)](#)) is 62.5 nm, in good agreement with the measured value. The pulse taken directly at the OC (inset of [Fig. 4\(a\)](#)) has a FWHM duration of 1.55 ps and is normally chirped. This enables compression in a 1.1-m section of SMF, resulting in a nearly transform-limited pulse ([Fig. 4\(a\)](#)) with a duration of 64 fs, which is very close to the measured value.

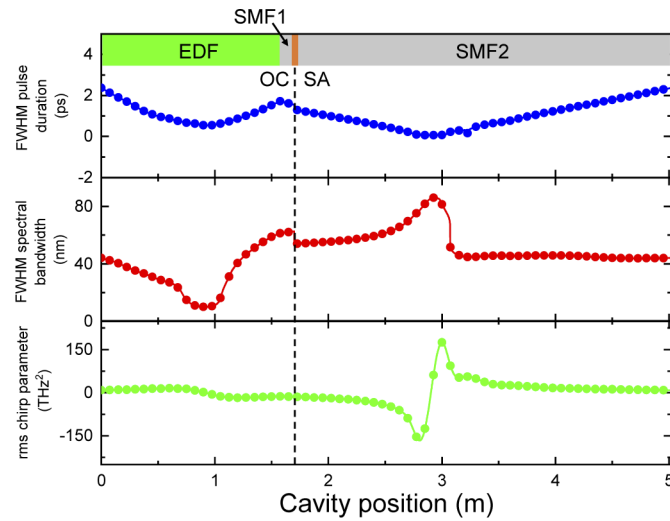


**Fig. 3.** Simulated evolutions of the FWHM temporal (blue) and spectral (red) widths and the rms chirp parameter (green) of the pulse along the cavity.

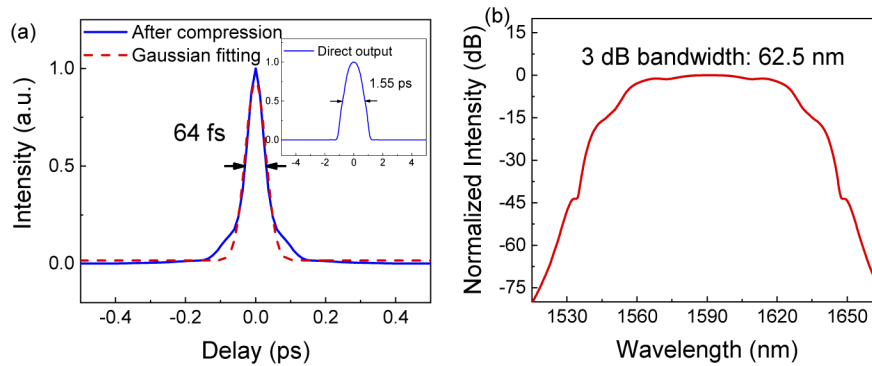


**Fig. 4.** (a) Simulated temporal intensity profiles of the compressed and direct output (inset) pulses. (b) Spectral intensity profile of the output pulse.

#### 4. Conclusions

We demonstrated a sub-70-fs stretched-pulse EDF laser that operates in the L band and requires only one gain segment. Mode locking of the laser is realised through the NPR effect by using a Brewster fibre grating as an in-fibre polariser. This laser delivers pulses at 40.63-MHz repetition rate and 1.59- $\mu\text{m}$  central wavelength that can be compressed externally to 64 fs. To our knowledge, this is the shortest duration obtained in L-band EDF lasers using a single gain segment. Our simple laser design lends itself well to all-fibre integration, and thus will be highly desirable for a variety of applications requiring L-band ultrashort pulses.

**Funding.** National Key Research and Development Program of China (2020YFB1805800); National Natural Science Foundation of China (61575120, 61975107); Natural Science Foundation of Shanghai (20ZR1471500); Overseas Expertise Introduction Project for Discipline Innovation (D20031); Key Laboratory of Space Active Opto-electronics Technology (2021-ZDKF-1); Engineering and Physical Sciences Research Council (EP/S003436/1 – PHOS).

**Disclosures.** The authors declare that there are no conflicts of interest related to this article.

**Data availability.** Data underlying the results presented in this paper are not publicly available at this time but may be obtained from the authors upon reasonable request.

**Supplemental document.** See [Supplement 1](#) for supporting content.

## References

1. W. Fu, L. G. Wright, P. Sidorenko, S. Backus, and F. W. Wise, "Several new directions for ultrafast fiber lasers [Invited]," *Opt. Express* **26**(8), 9432–9463 (2018).
2. M. E. Fermann and I. Hartl, "Ultrafast fibre lasers," *Nat. Photonics* **7**(11), 868–874 (2013).
3. X. Dong, P. Shum, N. Q. Ngo, C. C. Chan, B.-O. Guan, and H.-Y. Tam, "Effects of active fiber length on the tunability of erbium-doped fiber ring lasers," *Opt. Express* **11**(26), 3622–3627 (2003).
4. M. Fernandez-Vallejo, D. Ardanaz, and M. López-Amo, "Optimization of the Available Spectrum of a WDM Sensors Network Using a Mode-Locked Laser," *J. Lightwave Technol.* **33**(22), 4627–4631 (2015).
5. H. Kawagoe, S. Ishida, M. Aramaki, Y. Sakakibara, E. Omoda, H. Kataura, and N. Nishizawa, "Development of a high power supercontinuum source in the 1.7  $\mu\text{m}$  wavelength region for highly penetrative ultrahigh-resolution optical coherence tomography," *Biomed. Opt. Express* **5**(3), 932–943 (2014).
6. F. Morin, F. Druon, M. Hanna, and P. Georges, "Microjoule femtosecond fiber laser at 1.6  $\mu\text{m}$  for corneal surgery applications," *Opt. Lett.* **34**(13), 1991–1993 (2009).
7. K. Guesmi, Y. Meng, A. Niang, P. Mouchel, M. Salhi, F. Bahloul, R. Attia, and F. Sanchez, "1.6  $\mu\text{m}$  emission based on linear loss control in a Er:Yb doped double-clad fiber laser," *Opt. Lett.* **39**(22), 6383–6386 (2014).
8. Y. Meng, M. Salhi, A. Niang, K. Guesmi, G. Semaan, and F. Sanchez, "Mode-locked Er:Yb-doped double-clad fiber laser with 75-nm tuning range," *Opt. Lett.* **40**(7), 1153–1156 (2015).
9. Y. Meng, A. Niang, K. Guesmi, M. Salhi, and F. Sanchez, "1.61  $\mu\text{m}$  high-order passive harmonic mode locking in a fiber laser based on graphene saturable absorber," *Opt. Express* **22**(24), 29921–29926 (2014).
10. Y. Meng, G. Semaan, M. Salhi, A. Niang, K. Guesmi, Z.-c. Luo, and F. Sanchez, "High power L-band mode-locked fiber laser based on topological insulator saturable absorber," *Opt. Express* **23**(18), 23053–23058 (2015).
11. K. Tamura, E. P. Ippen, H. A. Haus, and L. E. Nelson, "77-fs pulse generation from a stretched-pulse mode-locked all-fiber ring laser," *Opt. Lett.* **18**(13), 1080–1082 (1993).
12. S. K. Turitsyn, B. G. Bale, and M. P. Fedoruk, "Dispersion-managed solitons in fibre systems and lasers," *Phys. Rep.* **521**(4), 135–203 (2012).
13. W. H. Renninger, A. Chong, and F. W. Wise, "Pulse Shaping and Evolution in Normal-Dispersion Mode-Locked Fiber Lasers," *IEEE J. Sel. Top. Quantum Electron.* **18**(1), 389–398 (2012).
14. Y. Song, C. Kim, K. Jung, H. Kim, and J. Kim, "Timing jitter optimization of mode-locked Yb-fiber lasers toward the attosecond regime," *Opt. Express* **19**(15), 14518–14525 (2011).
15. D. Y. Tang and L. M. Zhao, "Generation of 47-fs pulses directly from an erbium-doped fiber laser," *Opt. Lett.* **32**(1), 41–43 (2007).
16. F. Ö. Ilday, F. W. Wise, and T. Sosnowski, "High-energy femtosecond stretched-pulse fiber laser with a nonlinear optical loop mirror," *Opt. Lett.* **27**(17), 1531–1533 (2002).
17. X. Jin, G. Hu, M. Zhang, Y. Hu, T. Albrow-Owen, R. C. T. Howe, T.-C. Wu, Q. Wu, Z. Zheng, and T. Hasan, "102 fs pulse generation from a long-term stable, inkjet-printed black phosphorus-mode-locked fiber laser," *Opt. Express* **26**(10), 12506–12513 (2018).
18. J. Sotor, I. Pasternak, A. Krajewska, W. Strupinski, and G. Sobon, "Sub-90 fs a stretched-pulse mode-locked fiber laser based on a graphene saturable absorber," *Opt. Express* **23**(21), 27503–27508 (2015).
19. F. Ö. Ilday, J. Chen, and F. X. Kärtner, "Generation of sub-100-fs pulses at up to 200 MHz repetition rate from a passively mode-locked Yb-doped fiber laser," *Opt. Express* **13**(7), 2716–2721 (2005).
20. D. Deng, L. Zhan, Z. Gu, Y. Gu, and Y. Xia, "55-fs pulse generation without wave-breaking from an all-fiber Erbium-doped ring laser," *Opt. Express* **17**(6), 4284–4288 (2009).
21. D. Ma, Y. Cai, C. Zhou, W. Zong, L. Chen, and Z. Zhang, "37.4 fs pulse generation in an Er: fiber laser at a 225 MHz repetition rate," *Opt. Lett.* **35**(17), 2858–2860 (2010).
22. X. Li, W. Zou, and J. Chen, "34.3 fs pulse generation in an Er-doped fibre laser at 201 MHz repetition rate," *Electron. Lett.* **51**(4), 351–352 (2015).
23. M. Melo, O. Frazão, A. L. J. Teixeira, L. A. Gomes, J. R. Ferreira da Rocha, and H. M. Salgado, "Tunable L-band erbium-doped fibre ring laser by means of induced cavity loss using a fibre taper," *Appl. Phys. B* **77**(1), 139–142 (2003).
24. D. Yan, X. Li, S. Zhang, M. Han, H. Han, and Z. Yang, "L-band wavelength-tunable dissipative soliton fiber laser," *Opt. Express* **24**(2), 739–748 (2016).
25. Z. Wang, K. Qian, X. Fang, C. Gao, H. Luo, and L. Zhan, "Sub-90 fs dissipative-soliton Erbium-doped fiber lasers operating at 1.6  $\mu\text{m}$  band," *Opt. Express* **24**(10), 10841–10846 (2016).
26. Z. Wang, L. Zhan, X. Fang, C. Gao, and K. Qian, "Generation of Sub-60 fs Similaritons at 1.6  $\mu\text{m}$  From an All-Fiber Er-Doped Laser," *J. Lightwave Technol.* **34**(17), 4128–4134 (2016).
27. X. Wang, Y.-g. Liu, Z. Wang, Z. Wang, and G. Yang, "L-Band Efficient Dissipative Soliton Erbium-Doped Fiber Laser With a Pulse Energy of 6.15 nJ and 3 dB Bandwidth of 47.8 nm," *J. Lightwave Technol.* **37**(4), 1168–1173 (2019).
28. K. Zhou, G. Simpson, X. Chen, L. Zhang, and I. Bennion, "High extinction ratio in-fiber polarizers based on 45° tilted fiber Bragg gratings," *Opt. Lett.* **30**(11), 1285–1287 (2005).

29. C. Mou, H. Wang, B. G. Bale, K. Zhou, L. Zhang, and I. Bennion, "All-fiber passively mode-locked femtosecond laser using a 45°-tilted fiber grating polarization element," *Opt. Express* **18**(18), 18906–18911 (2010).
30. X. Liu, H. Wang, Z. Yan, Y. Wang, W. Zhao, W. Zhang, L. Zhang, Z. Yang, X. Hu, X. Li, D. Shen, C. Li, and G. Chen, "All-fiber normal-dispersion single-polarization passively mode-locked laser based on a 45°-tilted fiber grating," *Opt. Express* **20**(17), 19000–19005 (2012).
31. Z. Zhang, C. Mou, Z. Yan, K. Zhou, L. Zhang, and S. Turitsyn, "Sub-100 fs mode-locked erbium-doped fiber laser using a 45°-tilted fiber grating," *Opt. Express* **21**(23), 28297–28303 (2013).
32. J. Li, Z. Yan, Z. Sun, H. Luo, Y. He, Z. Li, Y. Liu, and L. Zhang, "Thulium-doped all-fiber mode-locked laser based on NPR and 45°-tilted fiber grating," *Opt. Express* **22**(25), 31020–31028 (2014).
33. N. Kanagaraj, A. Theodosiou, J. Aubrecht, P. Peterka, M. Kamrádek, K. Kalli, I. Kašík, and P. Honzátko, "All fiber mode-locked thulium-doped fiber laser using a novel femtosecond-laser-inscribed 45°-plane-by-plane-tilted fiber grating," *Laser Phys. Lett.* **16**(9), 095104 (2019).
34. Z. Yan, C. Mou, K. Zhou, X. Chen, and L. Zhang, "UV-Inscription, Polarization-Dependant Loss Characteristics and Applications of 45°Tilted Fiber Gratings," *J. Lightwave Technol.* **29**(18), 2715–2724 (2011).
35. T. Wang, Z. Yan, Q. Huang, C. Zou, C. Mou, K. Zhou, and L. Zhang, "Mode-Locked Erbium-Doped Fiber Lasers Using 45° Tilted Fiber Grating," *IEEE J. Sel. Top. Quantum Electron.* **24**, 1–6 (2018).
36. C. Mou, K. Zhou, L. Zhang, and I. Bennion, "Characterization of 45°-tilted fiber grating and its polarization function in fiber ring laser," *J. Opt. Soc. Am. B* **26**(10), 1905–1911 (2009).
37. D. Y. Tang, L. M. Zhao, B. Zhao, and A. Q. Liu, "Mechanism of multisoliton formation and soliton energy quantization in passively mode-locked fiber lasers," *Phys. Rev. A* **72**(4), 043816 (2005).
38. H. A. Haus, "Mode-locking of lasers," *IEEE J. Sel. Top. Quantum Electron.* **6**(6), 1173–1185 (2000).